ADAPTIVE OPTICS CONTROL FOR LASER MATERIAL PROCESSING

S. Mauch [*], **J. Reger** [*], **E. Beckert** [**]

[*] *Control Engineering Group, Institute for Automation and Systems Engineering, Ilmenau University of Technology, Helmholzplatz 5, 98693 Ilmenau, Germany (e-mail: steffen.mauch@tu-ilmenau.de, reger@ieee.org)*

[**] *Fraunhofer Institute for Applied Optics and Precision Engineering (IOF), Albert-Einstein-Str. 7, 07745 Jena, Germany (e-mail: erik.beckert@iof.fraunhofer.de)*

Abstract: An adaptive optics system is used for correcting tip-tilt disturbances in an experimental laser material processing setup. The proposed tip-tilt controller is based on PI-controllers that are fed with disturbance estimates from a Kalman-filter. In addition, delays due to wavefront computation in the wavefront sensor and from data transmission are taken into account in the loop-shaping design. Laboratory experiments demonstrate the practical usability of the presented approach.

Keywords: adaptive optics, tip-tilt control, Kalman-filtering, material processing

1. INTRODUCTION

In laser material processing, thermal lenses and abberations frequently are causes for problems due to its deteriorating effects on the wavefront. In course of these disturbances, processing results often are not as accurate as desired. Furthermore, costly increases of power supply may be necessary for processing the material due to the defocus of the laser beam. To tackle these issues, adaptive optics (AO) may be considered appropriate means for achieving a realtime correction of the disturbed wavefronts. AO have received attention for many years in astronomy (Meimon *et al.*, 2010; John W. Hardy, 1998; Francois Roddier, 1999) for increasing the image quality until the diffraction-limit spot.

In laser material processing, however, research is still in its infancy. First steps in this area have been conducted by *Fraunhofer Institute for Applied Optics and Precision Engineering (IOF)* Jena within the *KD OptiMi*[1] project line from 2010 until 2011. Within this research framework, an experimental setup, including a deformable mirror (C. Bruchmann *et al.*, 2012), was developed for increasing the beam quality in material processing with high power lasers.

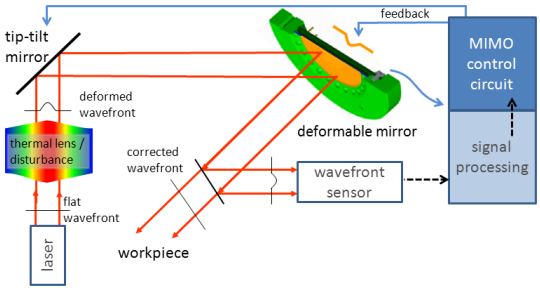

Fig. 1. wavefront correction setup

In the underlying paper, we contribute to the tip-tilt control, which is considered one of the most important deformations in high power laser applications (Ivo Buske, 2005). To this end, we use the experimental setup depicted in Fig. 1. The wavefront is monitored with a Shack-Hartmann wavefront sensor (WFS) that outputs the slopes in x- and y-direction of each subaperture. The sensor is connected to a real-time control system which calculates the wavefront so as to minimize the measured wavefront error and to compensate

[1] *KD OptiMi* is an excellence initiative supported by the German Federal Ministry of Education and Research (BMBF) and the state of Thuringia in Germany.

for the aberration. As may be concluded from Fig. 1, it is not possible to measure the disturbance directly, that is, the effect of the tip-tilt and deformable mirror is always superposed. In light of this problem, we propose the use of an integral controller and an observer for guessing the disturbance to the end of compensating for the tip-tilt deformations in the wavefront. The controller design also takes into account delays that originate from computations in the wavefront sensor and from the network transport to the control unit.

The paper is organized as follows: Section 2 starts with a brief description of the experimental setup. In Section 3, the system model for the tip-tilt mirror is explained. The main contributions of the paper are given in Sections 4 and 5. A control and estimation strategy is proposed which is apt for handling steplike disturbances. Section 6 is devoted to the conclusions and describes some forthcoming works.

2. EXPERIMENTAL SETUP

The experimental setup consists of a helium-neon (HeNe) laser with 632nm, a deformable mirror developed in-house by Fraunhofer IOF, a tip-tilt mirror S-330.2SL from Physik Instruments (PI), a Shack-Hartmann wavefront sensor, and a National Instruments LabVIEW PXI realtime-system; see Fig. 2 for the system setup. For testing purposes, usually, a low power laser is used. However, some tests for examination of the thermal behavior where already done with a 250W faserlaser. The tip-tilt mirror has an aperture of $d = 31.5$mm. The Shack-Hartmann wavefront sensor used is a HASO 3 Fast from Imagine Optic, which is capable to deliver about 905 frames per second and provides a CameraLink interface. As realtime system the PXI-8110 is used which receives the slopes through Gigabit Ethernet from another computer where the calculation of the slopes is done. Due to the slope calculations and the data transfer over Ethernet, there is a delay of about

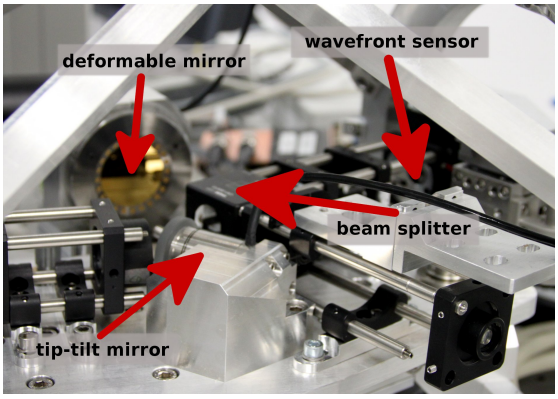

Fig. 2. complete system setup

3 msec. The tip-tilt mirror incorporates a built-in amplifier. The tip-tilt axis is rotated 45 degrees with respect to the wavefront sensor, due to the mounting, and therefore there is a coupling in the channels for the WFS. Consequently, it is not possible to use two separated controllers for controlling tip and tilt individually as it is done in standard approaches (Roddier, 1999). The control algorithm is compiled from a MATLAB/Simulink model via Simulink Coder, formerly Real-Time Workshop, and is then included in the LabVIEW PXI system.

3. TIP-TILT MIRROR MODEL

In AO the transient behavior of the piezoelectric actuators often is modeled as a first-order plant, see (Pachter *et al.*, 2002). This is possible when neglecting the amplifier characteristics. However in our setup, the amplifier has also to be taken into account. The frequency response of the mirror was measured directly with a scanning vibrometer PSV-400 from Polytec. Such-like scanning vibrometers measure the velocity of specified points for distinct frequencies on the mirror. With the relation $v = \dot{s}$, where s is the deflection, it is then possible to obtain the Bode plot, shown in Fig. 3, for the transfer function $G(s) = \frac{Y(s)}{U(s)}$, where $Y(s)$ is the deflection and $U(s)$ the input voltage of the amplifier.

It is also possible to measure the absolute displacement directly, but due to accumulating measurement errors, the result will not be reliable as with the velocity measurement. However, the transient behavior of a step may be monitored and compared with the determined frequency model. By means of the ARX algorithm, implemented in MATLAB System Identification toolbox, the transfer function

$$G(s) = \frac{514.9}{s^3 + 6432s^2 + 2.378e^7 s + 1.584e^{10}} \quad (1)$$

is identified out of the Fig. 3. The system is of third order for both tip and tilt, and shows to be stable and minimum phase. The resonance frequencies visible in the Bode plots are due to mechanical requirements in the measurement stage and do not occur in the final setup with appropriate attachment.

4. CONTROL ARCHITECTURE

Since the relationship between control voltage and mirror deformation is assumed linear, we may determine the actuator influence function from the steady-state behavior of the tip-tilt mirror also in a linear way. To this end, we use the same mechanisms which are employed for deformable

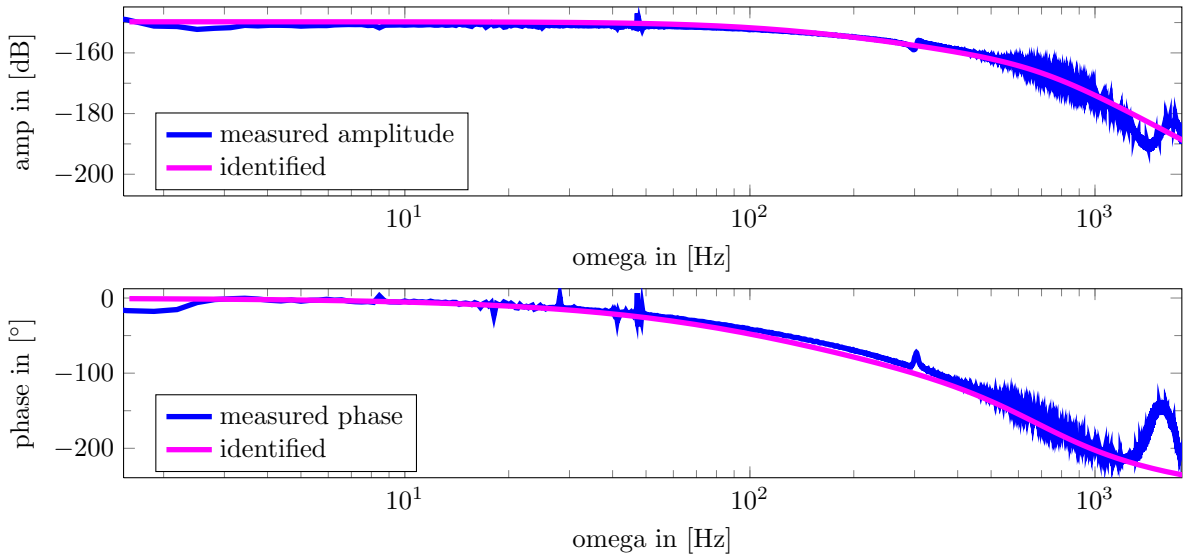

Fig. 3. Bode plot of the tip-tilt mirror

mirrors, e.g. see (Pachter *et al.*, 2002; Hardy, 1998).

In our setup, we have two actuators such that the phase distortion may be modeled as

$$\Phi(x,t) = \sum_{k=1}^{2} I_k(x,t) v_k(t)\,, \tag{2}$$

where $v_k(t)$ is the voltage applied to the k-th actuator at time t, x is the vector of coordinates, $I_k(x,t)$ is the contribution of the actuator to the phase and $\Phi(x,t)$ is representing the complete wavefront at time t. The wavefront may also be represented as a linear combination of Zernike polynomials, see Tab. 1.

i	$Z_i(r,\theta)$	name
0	1	piston
1	$2(\frac{r}{R})\cos(\theta)$	tip
2	$2(\frac{r}{R})\sin(\theta)$	tilt
3	$\sqrt{3}[2(\frac{r}{R})^2 - 1]$	focus
4	$\sqrt{6}(\frac{r}{R})^2\sin(2\theta)$	astigmatism
5	$\sqrt{6}(\frac{r}{R})^2\cos(2\theta)$	astigmatism

Table 1. low order Zernike polynomials

These polynomials are a sequence of polynomials which are orthogonal on the unit disk (Fig. 4).

The wavefront may then be described as

$$\Phi(x,t) = \sum_{i} a_i(t) Z_i(x) \tag{3}$$

where i is the number of Zernike coefficients $a_i\,(t)$ employed and x refers to polar coordinates, see Tab. 1.

Dealing with tip and tilt mode here, we have $i = 1, 2$, and its exactly these two modes which the tip-tilt mirror offers as degrees of freedom. The first Zernike mode $i = 0$ (piston mode) cannot be affected by the the tip-tilt mirror and

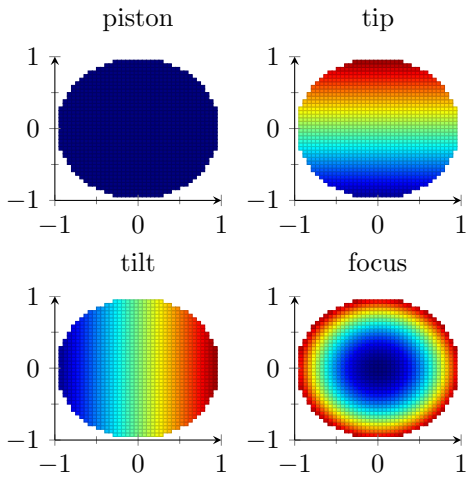

Fig. 4. illustration of principal Zernike modes

is dropped because it is unimportant for the underlying application.

The WFS has 14×14 apertures and delivers slopes in x- and y-direction. Therefore, for the output vector z of the WFS we have $z \in \mathbb{R}^{2\cdot196\times1}$. If the actuator u is deflected and z is stored column-wise in a matrix $M \in \mathbb{R}^{2\cdot196\times2}$ then we have a linear stationary relation between u and z, i.e. $M\,u = z$. We calculate the voltage $u \in \mathbb{R}^{2\times1}$ that is necessary for compensation of the distortion by resorting to the left inverse $M^+ = (M^{\mathrm{T}}M)^{-1}M^{\mathrm{T}}$, that is, $u = M^+ z$.

Due to the afore-mentioned couplings—rotational offset of the WFS axes to those of the tip-tilt mirror—using just PI-controllers turns out not to be sufficient. For compensating the delay, furthermore, a Smith-predictor may be conceived helpful. However, this approach also turns out to be inappropriate here because the delay is not well-known and also subject to stochastical changes.

For this reason, we opted for using an observer to decouple the system and regulate to the guessed value of the distortion. For reason of the stochastic nature of the distortion, generally, and the uncertainty in the tip-tilt model, a Kalman-filter is used in our approach.

4.1 Kalman-Filter Approach

We adhere to a linear state space representation of the system, for simplicity and for issues of implementation, in discrete time (Brian D. O. Anderson and John B. Moore, 2005) [2]

$$x_k = F_k x_{k-1} + G_k u_{k-1} + w_{k-1} \tag{4}$$
$$z_k = H_k x_k + v_k \tag{5}$$
$$v_k \in \mathcal{N}\{0, R_k\}\ ;\ w_k \in \mathcal{N}\{0, Q_k\} \tag{6}$$

where $k \in \mathbb{N}_0$ and $x_k \in \mathbb{R}^n$ is the state vector, $u_k \in \mathbb{R}^p$ the input vector, $w_k \in \mathbb{R}^n$ the unknown system noise, $v_k \in \mathbb{R}^q$ the unknown measurement noise, $F_k \in \mathbb{R}^{n\times n}$ the state transition matrix, $G_k \in \mathbb{R}^{n\times p}$ the input matrix, $H_k \in \mathbb{R}^{q\times n}$ the measurement matrix, and $z_k \in \mathbb{R}^q$ the output with additive noise. Due to numerical problems induced by rounding errors a modified version, named Joseph Kalman-Filter is used (Grewal and Andrews, 2008). This version shows more computational burden, but the respective covariance matrices better preserve symmetry and positive definiteness. The algorithm is as follows:

Initial values:

$$\hat{x}_0 = E\{x_0\}$$
$$P_0 = E\left\{[x_0 - \hat{x}_0][x_0 - \hat{x}_0]^{\mathrm{T}}\right\}$$

Estimation:

$$\hat{x}_k^- = F_k \hat{x}_{k-1} + G_k u_{k-1}$$
$$P_k^- = F_k P_{k-1} F_k^{\mathrm{T}} + Q_k$$

Propagation:

$$K_k = P_k^- H_k^T (H_k P_k^- H_k^{\mathrm{T}} + R_k)^{-1}$$
$$\hat{x}_k^+ = \hat{x}_k^- + K_k(z_k - H_k x_k^-)$$
$$P_k^+ = (I - K_k H_k) P_k^- - P_k^- H_k^T K_k^T + K_k(H_k P_k^- H_k^T + R_k) K_k^T$$

As initial value of P_0 we chose a diagonal matrix with large entries and $\hat{x}_0$ as a zero vector.

The coupling between the tip-tilt and the WFS is given by

$$\begin{pmatrix} x_{\mathrm{WFS}} \\ y_{\mathrm{WFS}} \end{pmatrix} = \sqrt{2} \begin{pmatrix} -0.5 & 0.5 \\ -0.5 & -0.5 \end{pmatrix} \begin{pmatrix} x_{\mathrm{tiptilt}} \\ y_{\mathrm{tiptilt}} \end{pmatrix} \tag{7}$$

which is validated by measurements. In (9) it is used for determining H.

[2] In F_k, G_k, and H_k we will later on drop the index k because of the time-invariance of the underlying process.

The augmented continuous-time state space system needed for Kalman-Filter may be described as:

$$\dot{x} = \begin{pmatrix} A_{\mathrm{tip}} & 0 & \dots & 0 \\ 0 & A_{\widehat{\mathrm{tip}}} & \ddots & \vdots \\ \vdots & \ddots & A_{\mathrm{tilt}} & 0 \\ 0 & \dots & 0 & A_{\widehat{\mathrm{tilt}}} \end{pmatrix} x + \begin{pmatrix} B_{\mathrm{tip}} & 0 \\ 0 & 0 \\ 0 & B_{\mathrm{tilt}} \\ 0 & 0 \end{pmatrix} u, \tag{8}$$

$$y = \frac{\sqrt{2}}{2} \begin{pmatrix} -\frac{1}{G(0)} x_1 - x_4 + \frac{1}{G(0)} x_7 + x_{10} \\ -\frac{1}{G(0)} x_1 - x_4 - \frac{1}{G(0)} x_7 - x_{10} \end{pmatrix} \tag{9}$$

where $A_{\mathrm{tip/tilt}}, B_{\mathrm{tip/tilt}}$ are the state-space representations of $G(s)$ from (1) in controller normal form. The transfer function from u to y regarding the model (8) and (9) is normalized to one because the left inverse M^+ handles the gain already.

The afore-presented continuous-time models have been discretized via bilinear transform (Tustin's method) with a sampling time of 0.75 msec for simulating the system and also for the implementation on the real-time hardware.

5. SIMULATIONS AND EXPERIMENTS

The disturbance is assumed as quasi-static, e.g. like thermal lenses whose properties vary very little with time. In the simulation as well as in the experiment we investigate the responses on step-like disturbances. In the experiment, a deformable mirror was used to generate well-defined tip-tilt disturbances. The deformable mirror may be considered fast enough such that the assumption of a step is a valid approximation. Naturally, in contrast to the simulation the step slope in the experiment is not as steep as in the simulation.

For the purpose of modeling the disturbance we use $A_{\widehat{\mathrm{tip}}}$ and $A_{\widehat{\mathrm{tilt}}}$ for approximating the step in state space. The eigenvalues read -1, -90, -100.

We assume white noise on the measurement with $\sigma = 5 \cdot 10^{-5}$ and $R_k = \mathrm{diag}(0.0005, 0.0005)$. The model uncertainty is assumed as

$$Q_k = \mathrm{diag}(0, 0, 0, 25, 5, 10, 0, 0, 0, 25, 5, 10).$$

In Fig. 5 simulation results are shown. From the first sub-figure we conclude that the guessed disturbance matches the real disturbance quite well. The disturbances are guessed in non-rotated coordinates. At 0.1 sec the estimated tilt, as well as tip at 0.3 sec, has an overshoot which is due to the delay of the WFS and the model uncertainty. Subfigure two shows the difference between guessed and measured tip-tilt, sub-figures three and four

the tip-tilt values first in original and the second in rotated coordinates. Sub-figure four depicts the coupling. Hence, when subject to coupling, for compensation of tip/tilt both actuators have to be driven.

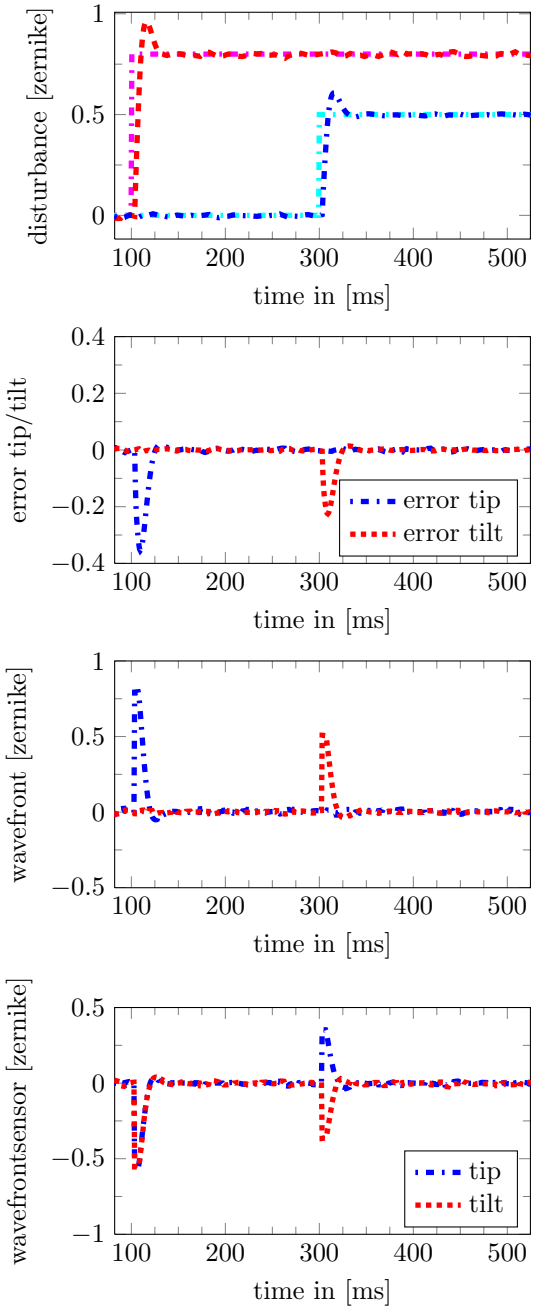

Fig. 5. simulation results

The PI controller is devised via the complementary sensitivity $T(s) = \frac{Y(s)}{R(s)}$, see Fig. 6 for the corresponding block diagram. However, if striving for performance the effect of rotation can be neglected in the design, thus, a simplified loop may be assumed, see Fig. 7. For simplicity in the design, the discrete-time stationary-gain Kalman-Filter is converted to continuous time via bilinear transformation.

These considerations lead to

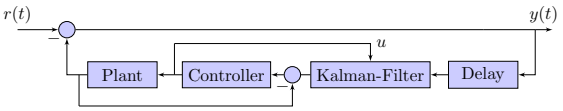

Fig. 6. block diagram of the control loop

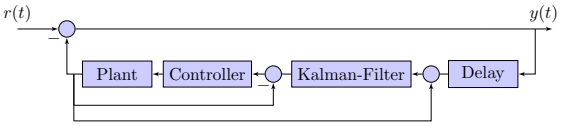

Fig. 7. simplified block diagram of the control loop

$$T(s) = \frac{1 + C(s)G(s)\,(1 - G_{\mathrm{KF}}(s))}{1 + C(s)G(s)\,(1 - G_{\mathrm{KF}}(s) + G_{\mathrm{KF}}(s)e^{-sT_{\mathrm{d}}})} \tag{10}$$

where T_{d} is the delay and $G_{\mathrm{KF}}(s)$ is the transfer function of the Kalman-Filter when the gain has reached its stationary value after approximately 50 msec. The stationary gain P_∞ results from the algebraic Riccati equation [3]

$$\begin{aligned} P_\infty &= F_{\widehat{\mathrm{tip}}} P_\infty F_{\widehat{\mathrm{tip}}}^{\mathrm{T}} + Q \\ &- F_{\widehat{\mathrm{tip}}} P_\infty C_{\widehat{\mathrm{tip}}}^{\mathrm{T}} (C_{\widehat{\mathrm{tip}}} P_\infty C_{\widehat{\mathrm{tip}}}^{\mathrm{T}} + R)^{-1} C_{\widehat{\mathrm{tip}}} P_\infty F_{\widehat{\mathrm{tip}}}^{\mathrm{T}} \end{aligned} \tag{11}$$

with $F_{\widehat{\mathrm{tip}}}$ as discretized matrix $A_{\widehat{\mathrm{tip}}}$ and $C_{\widehat{\mathrm{tip}}} = \begin{pmatrix} 1 & 0 & 0 \end{pmatrix}$. This is leading to the gain

$$K_\infty = \begin{pmatrix} 0.1542 & -0.0122 & -2.8087 \end{pmatrix}^{\mathrm{T}}.$$

For choosing a controller, we refer to the approximate open loop transfer function

$$L(s) = C(s)G(s)\left(1 - G_{\mathrm{KF}}(s) + G_{\mathrm{KF}}(s)e^{-sT_{\mathrm{d}}}\right)$$

with $C(s) = K_{\mathrm{p}}\frac{1+\tau s}{s}$ which satisfies the two following equations

$$|L(i\omega_c)| \stackrel{!}{=} 1 \tag{12}$$

and

$$\arg\{L(i\omega_c)\} = -\pi + \frac{85\pi}{180} \tag{13}$$

Thus, we design the controller for the nominal complementary sensitivity

$$\tilde{T}(s) = \frac{L(s)}{1 + L(s)}$$

instead of $T(s)$ from (10). The design leads to an acceptable approximation, see Fig. 8.

We selected cut-off frequency $\omega_c = 160\,\mathrm{rad/sec}$, subsequently, τ is calculated by solving equation (13). The phase margin was specified as 85° because of the robustness and overshoot aspect. K_{p} is determined with equation (12). The resulting controller reads:

$$C(s) = \frac{198.1469230(1 + 0.003227017369s)}{s}.$$

[3] Due to the same underlying matrices, notation $\widehat{\mathrm{tip}}$ may be replaced with $\widehat{\mathrm{tilt}}$.

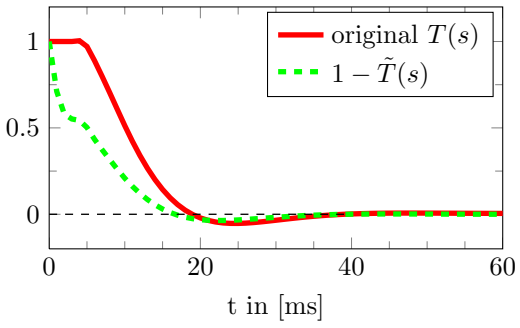

Fig. 8. step response of the closed-loop system

The designed observer and controller was compiled with the real-time workshop from a Simulink model and then used as DLL in the PXI system. Fig. 9 depicts the experimental results.

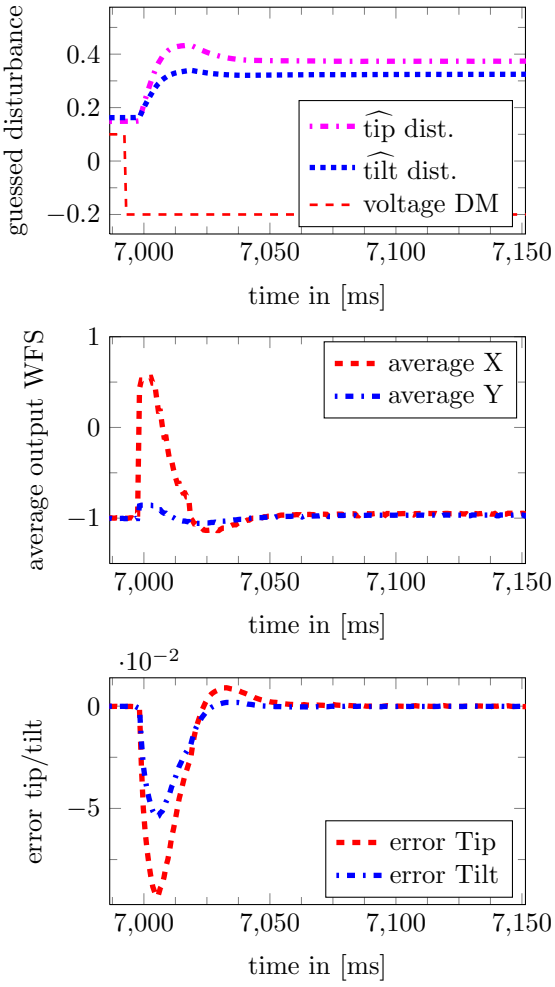

Fig. 9. experimental results

At 7 sec the deformable mirror is used to change the tip-tilt behavior as to be seen in sub-figure one. The same overshoot is apparent in the estimated disturbance as in the simulation sub-figure 1 in Fig. 5. Sub-figure two shows the average output of the WFS slopes in x and y direction. When applying the tip-tilt correction, the same average value should be reached, here about -1. This is achieved at approximately 20 msec which is also the result of the simulation. Sub-figure three shows the difference between estimated disturbance and measured disturbance.

6. CONCLUSIONS

We have devised a robust controller for the tip-tilt disturbance correction in an experimental AO system. In the experimental setup, the handling of model uncertainty and the delay play a crucial role. Classical loop shaping ideas are combined with a Kalman-Filter based estimation scheme. The developed design leads to satisfactory simulation results when the system is subject to step-wise disturbances. Conducted laboratory experiments mimic the simulation results.

Future work will concentrate on the control of the deformable mirror in a MIMO-setup. Furthermore, experiments with disturbances of richer dynamics will be carried out such that different control strategies, as for example $\mathcal{H}_2$ and $\mathcal{H}_\infty$ optimal control approaches, may be compared in a realistic setup. Also we intend to fully integrate the WFS into the realtime system so as to further reduce the delay for increasing the overall performance and reducing the computational burden.

7. ACKNOWLEDGMENTS

The authors express their gratitude to Roland Klein, Claudia Reinlein, and Michael Appelfelder of Fraunhofer IOF Jena for their support and to BMBF for granting *KD OptiMi2*.

REFERENCES

Brian D. O. Anderson and John B. Moore, 2005, Optimal Filtering, *Dover Publications*,Sec. 3.1

Ivo Buske, 2005, Aberrationen in Nd:YAG - Hochleistungslasern und -verstärkern: Ihr Einfluss und ihre Korrektur mit adaptiver Optik [in German], *Dissertation*, TU Berlin

Bruchmann, Appelfelder, Beckert, Eberhardt and Tünnerman, 2012, Thermo-mechanical properties of a deformable mirror with screen printed actuator, *(SPIE) Conference Series*,vol. 8253

Mohinder S. Grewal and Angus P. Andrews, 2008, Kalman Filtering: Theory and Practice Using MATLAB Edt. 3, *Wiley-IEEE Press*, 133-137

John W. Hardy, 1998, Adaptive Optics for Astronomical Telescopes (Oxford Series in Optical & Imaging Sciences), *Oxford University Press, USA*,chap. 2

Meimon, Serge and Petit, Cyril and Fusco, Thierry and Kulcsar, Caroline, 2010, Tip-tilt disturbance model identification for Kalman-based control scheme: application to XAO and ELT systems ,*Journal of the Optical Society of America*, A122–32

Pachter, Meir and Oppenheimer, Michael W., 2002, Adaptive optics for airborne platforms–Part 1: modeling, *Optics & Laser Technology 34*,143–158

Francois Roddier, 1999, Adaptive Optics in Astronomy, *Cambridge University Press*,chap. 2